Detection of Residual Brain Arteriovenous Malformations after Radiosurgery: Diagnostic Accuracy of Contrast-Enhanced Three-Dimensional Time of Flight MR Angiography at 3.0 Tesla

Kyoung Eun Lee, MD[1]
Choong Gon Choi, MD[1]
Jin Woo Choi, MD[1]
Byung Se Choi, MD[1]
Deok Hee Lee, MD[1]
Sang Joon Kim, MD[1]
Do Hoon Kwon, MD[2]

Index terms:
Brain
Arteriovenous malformation
Radiosurgery
Magnetic resonance (MR)
Angiography

DOI:10.3348/kjr.2009.10.4.333

Korean J Radiol 2009;10:333-339
Received December 10, 2008; accepted after revision March 2, 2009.

Departments of [1]Radiology, [2]Neurosurgery, Asan Medical Center, University of Ulsan College of Medicine, Seoul 138-736, Korea

Address reprint requests to:
Choong Gon Choi, MD, Department of Radiology, Asan Medical Center, University of Ulsan, 388-1 Poongnap-dong, Songpa-gu, Seoul 138-736, Korea.
Tel. (822) 3010-4374, 4352
Fax. (822) 476-4719
e-mail: cgchoi@amc.seoul.kr

Objective: Although three-dimensional time-of-flight magnetic resonance angiography (3D TOF-MRA) is used frequently as a follow-up tool to assess the response of arteriovenous malformations (AVMs) after radiosurgery, the diagnostic accuracy of 3D TOF-MRA is not well known. We evaluated the diagnostic accuracy of contrast-enhanced 3D TOF-MRA at 3.0 Tesla for the detection of residual AVMs.

Materials and Methods: This study included 32 AVMs from 32 patients who had been treated with radiosurgery (males/females: 21/11; average patient age, 33.1 years). The time interval between radiosurgery and MRA was an average of 35.3 months (range, 12–88 months). Three-dimensional TOF-MRA was obtained at a magnetic field strength of 3.0 Tesla after infusion of contrast media, with a measured voxel size of 0.40 × 0.80 × 1.4 (0.45) mm^3 and a reconstructed voxel size of 0.27 × 0.27 × 0.70 (0.05) mm^3 after zero-filling. X-ray angiography was performed as the reference of standard within six months after MRA (an average of two months). To determine the presence of a residual AVM, the source images of 3D TOF-MRA were independently reviewed, focusing on the presence of abnormally hyperintense fine tangled or tubular structures with continuity as seen on consecutive slices by two observers blinded to the X-ray angiography results.

Results: A residual AVM was identified in 10 patients (10 of 32, 31%) on X-ray angiography. The inter-observer agreement for MRA was excellent (κ = 0.813). For the detection of a residual AVM after radiosurgery as determined by observer 1 and observer 2, the source images of MRA had an overall sensitivity of 100%/90% (10 of 10, 9 of 10), specificity of 68%/68% (15 of 22, 15 of 22), positive predictive value of 59%/56% (10 of 17, 9 of 16), negative predictive value of 100%/94% (15 of 15, 15 of 16) and diagnostic accuracy of 78%/75% (25 of 32, 24 of 32), respectively.

Conclusion: The sensitivity of contrast-enhanced 3D TOF-MRA at 3.0 Tesla is high but the specificity is not sufficient for the detection of a residual AVM after radiosurgery.

A brain arteriovenous malformation (AVM) is an important cause of intracranial hemorrhage, especially in young adults and children (1). AVMs are usually treated with surgical resection, endovascular embolization, radiosurgery or a combination of these methods (1–5). Radiosurgery has been increasingly used for the treatment of small or residual AVMs after surgical resection or embolization. After radiosurgery, microvascular structures within the AVM begin

to be obliterated by endothelial cell damage and proliferation of smooth muscle cells, a process that usually continues for 2–3 years (6). Occasionally, complete obliteration of an AVM has been reported several years after radiosurgery (7–9). Recent studies have reported a decreased but still remaining risk of hemorrhage during the latency period (10, 11). Most physicians usually see patients at follow-up at a regular interval to evaluate the response to radiosurgery. As a follow-up imaging study, X-ray angiography is the gold standard to evaluate the response of an AVM to radiosurgery. However, invasiveness and potential neurological complications hinder the use of X-ray angiography in routine follow-up studies (12, 13). In many institutions, non-invasive magnetic resonance imaging (MRI) and magnetic resonance angiography (MRA) have been frequently used as follow-up tools to assess the response of AVMs and the adjacent brain parenchyma (14-16).

Three-dimensional time-of-flight (3D TOF) MRA is a commonly used technique for the delineation of an AVM nidus during the planning of radiosurgery. However, the diagnostic accuracy of 3D TOF-MRA for the detection of a residual AVM after radiosurgery is not well known. Previous studies with the use of the modality with a magnetic field strength of 1.5 Tesla (T) have just mentioned qualitatively the usefulness of 3D TOF-MRA for monitoring the nidal response after radiosurgery, but did not evaluate diagnostic performance of the technique quantitatively (14, 15). Only a study by Mukherji et al. (16) reported that the sensitivities of the use of 3D TOF-MRA for small AVMs (< 1 cm) were 27% and 50% for maximum intensity projection (MIP) and source images, respectively. Although 3D dynamic MRA is an emerging new technique, it has still limitations to detect a small residual AVM due to relatively low spatial resolution (17). Therefore, 3D TOF-MRA, which has higher spatial resolution than dynamic MRA, may be necessary to perform to evaluate a radiosurgically treated AVM in detail. In this study, we have attempted to determine whether contrast-enhanced 3D TOF-MRA obtained at 3.0 T is sufficiently accurate for the detection of a residual AVM after radiosurgery.

MATERIALS AND METHODS

Patients

Patients met the following inclusion criteria: a patient who had a brain AVM that was confirmed by conventional X-ray angiography, treated with radiosurgery and underwent both follow-up 3D TOF-MRA at 3.0 T and X-ray angiography. From August 2005 to March 2008, 34 patients were identified from an MRA and gamma-knife radiosurgery database. Two patients were excluded from consideration because of more than a six-month interval between follow-up MRA and X-ray angiography (seven and 11 months, respectively). The remaining 32 patients constituted the subjects for analysis in this study (males/females, 21/11; age range 12–52 years; average age, 33.1 years). Follow-up MRA was performed always prior to X-ray angiography. MRA and X-ray angiography were performed within six months (average interval, two months). Radiosurgery and follow-up MRA were performed within 12–88 months (average interval, 35.3 months).

Arteriovenous Malformation Characteristics and Treatment

The locations of 32 AVMs were the frontal lobe (n = 5), parietal lobe (n = 9), temporal lobe (n = 6), occipital lobe (n = 3), corpus callosum (n = 3), basal ganglia (n = 3), thalamus (n = 1), cerebellum (n = 1) and both the basal ganglia and the thalamus (n = 1). The mean volume of an AVM was 2.3 cm^3 (volume range, 0.1–11 cm^3). The volume of an AVM before radiosurgery was calculated by the use of GammaPlann software (version 5.3; Elekta Instrument, Stockholm, Sweden). All patients were treated using a Leksell gamma knife (Elekta Instrument) under local anesthesia. A stereotactic head frame was used for guiding and monitoring the treatment in all cases. Radiation doses were 20–25 Gy/50–65% isodose at the AVM margin. Thirteen patients were also treated by embolization with coils or glue before or after gamma knife radiosurgery.

Contrast-Enhanced 3D TOF-MRA and X-ray Angiography Techniques

All follow-up MRA was performed with the use of a 3.0 T MRI system (Achieva, Philips Medical Systems, Best, The Netherlands) using an 8-channel SENSE head coil. Axial T2* gradient echo images were first obtained to identify the presence or absence of a hemorrhagic event, with TR/TE 900/16 milliseconds, flip angle 20 degrees, slice thickness/gap 3/0 mm, slice number 30. Next, gadoterate meglumine (0.1 mmol/kg Dotarem; Guerbet, Roissy, France) was infused intravenously via the right antecubital vein by use of an auto-injector (Medras; Medrad, Indionola, PA) with an injection rate of 2–3 ml/sec followed by a 15–20 ml saline flush at the same rate. Contrast media was used to improve the visibility of small arteries or veins of a residual AVM. One minute after injection of contrast media, a 3D TOF-MRA scan was started with imaging parameters as follows: a three-

dimensional fast field echo sequence with repetition time/echo time, 25/3.45 milliseconds; flip angle, 20 degrees; field of view/rectangular field of view, 240 mm/80%; scan percentage, 50%; scan matrix/reconstruction matrix, 600/880; slice number/slice thickness/slice overlap, 114/1.4 mm/50%; SENSE factor, 2 (right-left direction); no vein saturation slab, magnetization transfer or fat saturation pulse; optimized non-saturating excitation (TONE) pulse; actual bandwidth, 108.6 Hertz/pixel. The imaging parameters utilized yielded a measured voxel size of 0.40 × 0.80 × 1.4 (0.45) mm^3 and a reconstructed voxel size of 0.27 × 0.27 × 0.70 (0.05) mm^3 after zero-filling of an 880 matrix along frequency and phase directions. The acquisition time was 4 minutes 26 seconds. A total of 114 slices were sampled in three slabs using CHARM (chunk acquisition and reconstruction method; Philips Medical Systems) to avoid venetian blind artifacts. The scan range was 80 mm and covered an AVM in the central portion of the scan range in most patients.

X-ray angiography was performed with use of a biplane Integris BN 3000 system (Philips Medical Systems). A 4-Fr headhunter catheter was introduced into the ascending aorta via the transfemoral route and was navigated into the carotid or vertebral artery. The appropriate carotid or vertebral artery was selected according to the decision of the angiographer. The intracranial arteries were displayed in at least two projections, i.e. anterior-posterior and lateral, by automatic injection of 6–8 mL of iodixanol (320 mg iodine/ml, Visipaque; Amersham, Cork, Ireland). X-ray angiography was performed with a 178 mm or 229 mm (7 or 9 inches) field of view and a 1,024 matrix, yielding a measured pixel size of 0.17 × 0.17 mm^2 or 0.22 × 0.22 mm^2, respectively. Our Institutional Review Board approved the study protocol and the requirement for patient written informed consent was waived.

Image Analysis

Two observers, a neuroradiologist who had more than 10 years experience in the interpretation of 3D TOF-MRA and a fourth year resident of radiology assessed the source images of 3D TOF-MRA independently and without knowledge of the follow-up X-ray angiography results. Special attention was paid to the presence or absence of abnormal vascular structures, suggestive of a residual AVM nidus or draining veins. Abnormal vascular structures were defined as abnormal hyperintense fine tangled structures or tubular structures with continuity as seen on consecutive slices. Irregular or nodular hyperintense lesions without a branching pattern were regarded as radiation-induced parenchymal enhancement (RIPE). Follow-up X-ray angiographic images were analyzed based on the consensus of an experienced neuroradiologist and a neurosurgeon with more than 10 years experience in the practice of neuroangiography and radiosurgery of AVMs, respectively. The absence of early draining veins was regarded as complete obliteration of an AVM. The presence of residual ectatic vessels or angiomatous changes around the obliterated nidus was not regarded as due to the presence of a residual AVM. The presence of an early draining vein with or even without a definitely visible nidus was regarded as incomplete obliteration or as due to a residual AVM. The volume of a residual AVM was estimated from the source images of 3D TOF-MRA by using a PACS (Picture Archiving and Communication System; Petavision, Asan Medical Center, Seoul). The inter-observer agreement rate was calculated by the use of kappa (κ) statistics and sensitivity, specificity, positive predictive value (PPV), negative predictive value (NPV) and diagnostic accuracy of 3D TOF-MRA for the detection of a residual AVM after radiosurgery were determined.

RESULTS

As depicted on follow-up X-ray angiography, 10 patients had a residual AVM nidus or early draining vein. The remaining 22 patients had no residual AVM. The mean volume of a residual AVM was 0.28 cm^3 (range 0.06–0.65 cm^3). For all patients, the quality of 3D TOF-MRA was adequate or sufficient for diagnosis. Inter-observer agreement of 3D TOF-MRA was excellent (κ = 0.813). As determined by observer 1 and observer 2, the source images of 3D TOF-MRA had overall sensitivity of 100%/90% (10 of 10, 9 of 10), specificity of 68%/68% (15 of 22, 15 of 22), PPV of 59%/56% (10 of 17, 9 of 16), NPV of 100%/94% (15 of 15, 15 of 16) and diagnostic accuracy of 78%/75% (25 of 32, 24 of 32), respectively, for the detection of a residual AVM nidus or draining veins after radiosurgery (Table 1).

Typical true positive and true negative cases are presented in Figures 1 and 2, respectively. With the use of 3D TOF-MRA, observers 1 and 2 considered seven and seven patients, respectively, as having a residual AVM, but the patients showed completely obliterated AVMs on follow-up X-ray angiography (Fig. 3). Of these patients, six patients showed overlapping findings. Observer 2 considered one patient as having complete obliteration with RIPE, but follow-up X-ray angiography demonstrated the presence of a residual AVM nidus with early draining veins (Fig. 4). This situation was due to an interpretation error by observer 2 and was the only false negative case as identified by both observers. The false positive and false negative results for the use of 3D TOF-MRA are

summarized in Table 2.

DISCUSSION

Our study showed that contrast-enhanced 3D TOF-MRA performed at 3.0 T has a high sensitivity (90–100%), but a relatively low specificity (68%) for the detection of a residual AVM after gamma-knife radiosurgery. The high sensitivity may be due to the improved spatial resolution of 3D TOF-MRA performed at 3.0 T (18, 19). The infusion of contrast media may also improve the vessel-background tissue contrast and the depiction of small vessel segments. These features allowed the sensitive detection of abnormal vascular structures that were suggestive of a residual AVM nidus or draining veins. Specificity was lower than expected due to the inclusion of eight patients with false-

Table 1. Comparison of 3D TOF-MRA with X-ray Angiography

		X-ray Angiography		
		Residual AVM	Obliterated AVM	Total
3D TOF-MRA by Observer 1	Residual AVM	10	7	17
	Obliterated AVM	0	15	15
	Total	10	22	32
3D TOF-MRA by Observer 2	Residual AVM	9	7	16
	Obliterated AVM	1	15	16
	Total	10	22	32

Note.— 3D TOF-MRA = three-dimensional time-of-flight magnetic resonance angiography, AVM = arteriovenous malformation

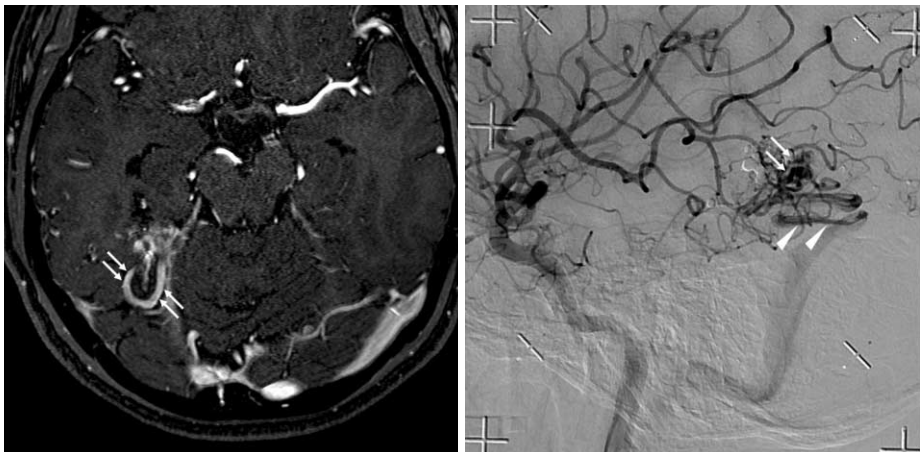

Fig. 1. Findings for typical true positive case. 45-year-old woman had ruptured arteriovenous malformation located at right medial temporo-occipital lobe and was treated with gamma-knife 46 months prior.
A. Source image of 3D TOF-MRA shows entangled tubular enhancing lesions (arrows) in right medial temporo-occipital lobe, which were interpreted as due to presence of residual arteriovenous malformation with draining vein by both observers.
B. Lateral view of right internal carotid angiogram demonstrates presence of residual arteriovenous malformation (arrows) with early draining vein (arrowheads).

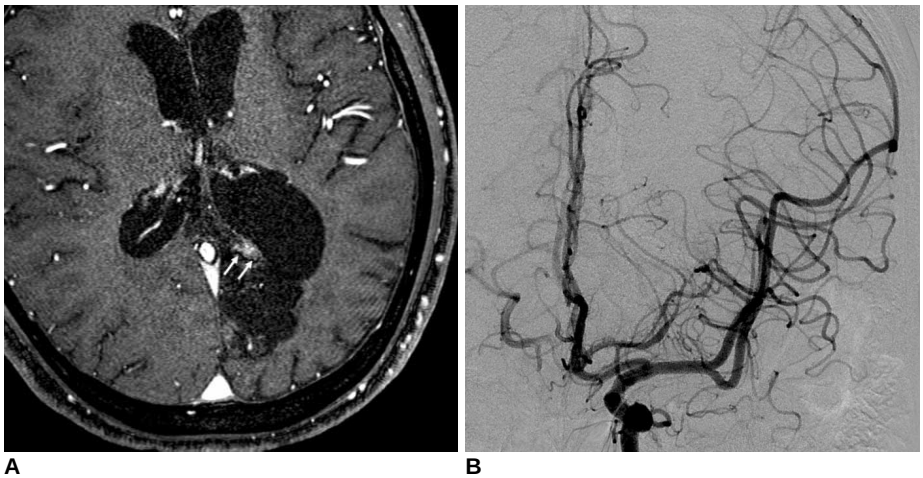

Fig. 2. Findings for typical true negative case. 21-year-old man had ruptured arteriovenous malformation located at left parietal lobe and was treated with gamma-knife 28 months prior.
A. Source image of 3D TOF-MRA shows large encephalomalatic change and focal mild brain parenchymal enhancement without branching pattern (arrows) in left medial parietal lobe, which was interpreted as due to complete obliteration of arteriovenous malformation by both observers.
B. On left internal carotid and vertebral angiogram (not shown here), no residual arteriovenous malformation or early draining vein is seen.

positive results from the use of 3D TOF-MRA (Table 2). In our experience, the most important cause of false positive results was the presence of persistent ectatic vessels around the obliterated nidus rather than RIPE. Frequently, residual ectatic vessels were mixed with RIPE and the resulting pattern mimicked a residual AVM. Residual ectasia of former afferent or efferent vessels can persist adjacent to an AVM, even after transnidus flow has been eliminated (20). These residual ectatic vessels can be misinterpreted as feeding arteries or as early draining veins that are suggestive of a residual AVM. This situation seems to be an unavoidable limitation of 3D TOF-MRA, which is not a dynamic study. The use of dynamic MRA can be added to 3D TOF-MRA to solve this kind of problem (17, 21). Sufficient spatial and temporal resolution to distinguish residual ectatic vessels with a true residual AVM is required. For dynamic MRA, temporal resolution should be less than one second to detect early draining veins

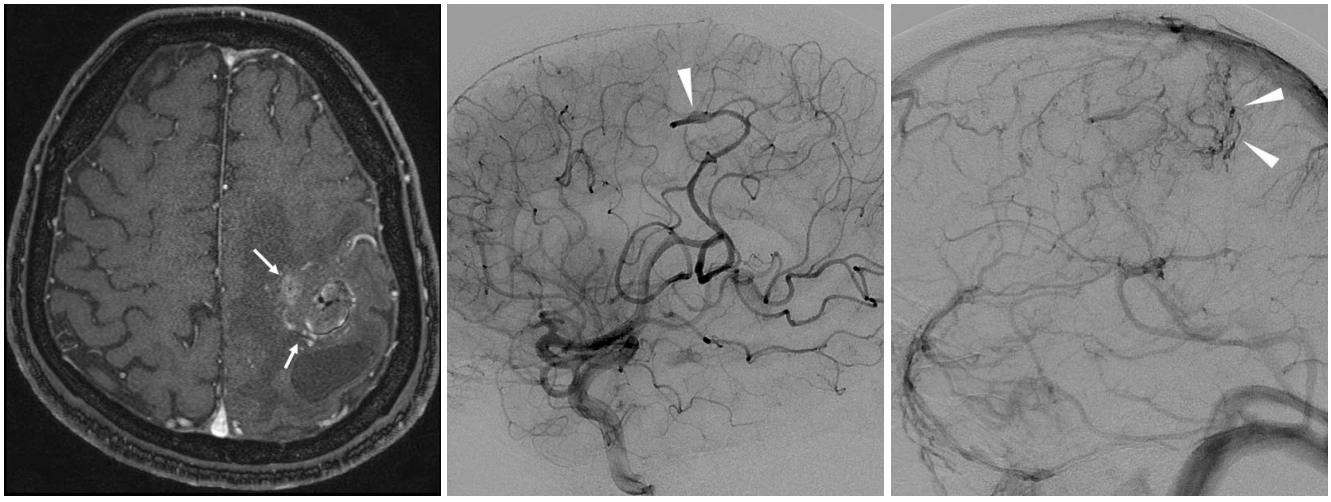

Fig. 3. Findings for false positive case. 51-year-old man had arteriovenous malformation located at left parietal lobe and was treated by gamma-knife 18 months prior.
A. Source image of 3D TOF-MRA shows irregular parenchymal enhancement and tubular enhancing vessels located at left parietal lobe (arrows). Both observers interpreted this case as due to presence of residual arteriovenous malformation.
B, C. On left internal carotid angiogram, no residual arteriovenous malformation is seen but still persistent ectasia of feeding artery and abnormal small vein (arrowheads) are seen.

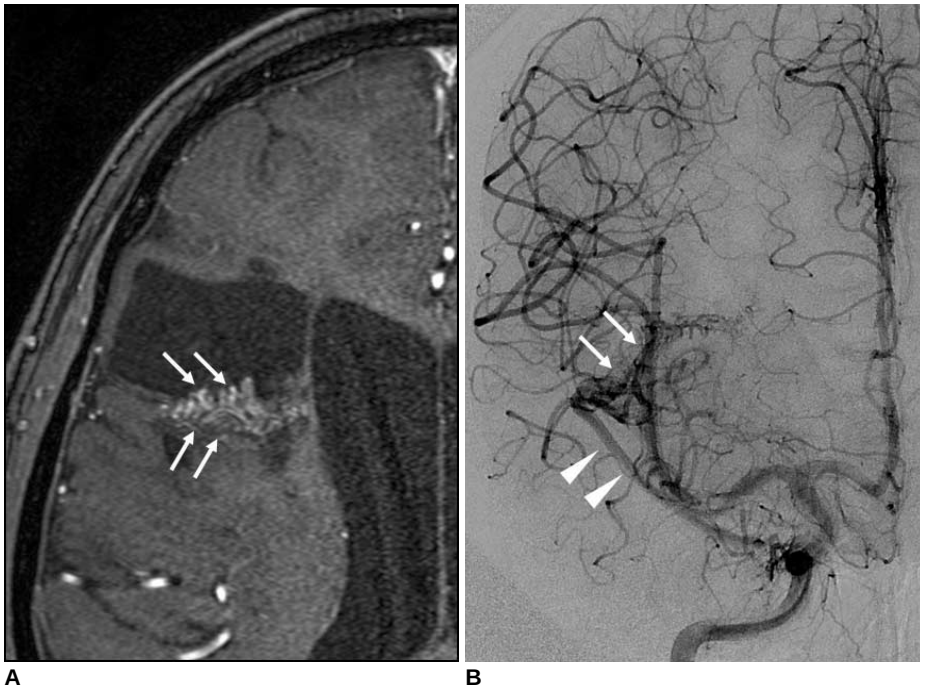

Fig. 4. Findings for false negative case by observer 2. 18-year-old woman had arteriovenous malformation at right frontal lobe and was treated by gamma-knife 88 months prior.
A. Source image of 3D TOF-MRA shows fine reticular enhancing lesion (arrows) located at posterior margin of encephalomalatic change. Observer 2 interpreted this case as due to complete obliteration of arteriovenous malformation with radiation change.
B. Right internal carotid angiogram demonstrates presence of residual arteriovenous malformation (arrows) with early draining vein (arrowheads).

Table 2. Summary of False Positive or False Negative Cases as Determined on 3D TOF-MRA

	Cases	Observer 1	Observer 2	X-ray Angiography	Estimated Causes
False Positive 1	M/51, left frontal lobe	Residual AVM	Residual AVM	Complete obliteration	Persistent ectatic vessels + RIPE
False Positive 2	M/53, right BG, thalamus	Residual AVM	Residual AVM	Complete obliteration	Persistent ectatic vessels + RIPE
False Positive 3	M/22, right frontal lobe	Residual AVM	Residual AVM	Complete obliteration	Persistent ectatic vessels + RIPE
False Positive 4	M/37, right thalamus	Residual AVM	Residual AVM	Complete obliteration	Persistent ectatic vessels + RIPE
False Positive 5	M/36, left frontal lobe	Complete obliteration	Residual AVM	Complete obliteration	Persistent ectatic vessels + RIPE
False Positive 6	F/12, right parietal lobe	Residual AVM	Residual AVM	Complete obliteration	Persistent ectatic vessels + RIPE
False Positive 7	M/43, left BG	Residual AVM	Residual AVM	Complete obliteration	Persistent ectatic vessels + RIPE
False Positive 8	F/43, right parietal lobe	Residual AVM	Complete obliteration	Complete obliteration	Persistent ectatic vessels + RIPE
False Negative 1	F/18, right frontal lobe	Residual AVM	Complete obliteration	Residual AVM	Interpretation error

Note.— AVM = arteriovenous malformation, BG = basal ganglia, RIPE = radiation-induced parenchymal enhancement

confidently. As spatial resolution of dynamic MRA is usually related reciprocally with temporal resolution, it may be difficult to detect a small residual AVM by the use of dynamic MRA with high temporal resolution. However, the combination of 3D TOF-MRA with dynamic MRA seems to be the current best option. Further investigations may be necessary to evaluate the role of the use of dynamic MRA for the detection of the small sized residual AVMs included in this study.

Another possible cause of false positive results of 3D TOF-MRA was the relatively long follow-up interval between the use of 3D TOF-MRA and X-ray angiography (with a maximum of six months). A small residual AVM could be obliterated during the follow-up period between the use of 3D TOF-MRA and X-ray angiography.

The high NPV of 3D TOF-MRA is of interest. In this study, only one false negative result of 3D TOF-MRA (Fig. 4) was obtained. Observer 2 interpreted the fine reticular enhancing lesion located at the posterior margin of encephalomalatic change as due to a radiation change. However, on a retrospective review, the source images showed the presence of clearly abnormal vessels with branching patterns on consecutive slices (an interpretation error of observer 2). This experience suggests that the interpreter should be careful in assessing the source images of 3D TOF-MRA to differentiate RIPE from a residual AVM. RIPE near or within the AVM nidus can be seen for several years, even after successful obliteration of an AVM (7). This situation may be due to disruption of the blood-brain barrier or may be due to radiation necrosis.

The high NPV of contrast-enhanced 3D TOF-MRA can decrease the need for X-ray angiography to confirm AVM obliteration. The use of X-ray angiography can be probably limited to patients who are suspected as having a residual AVM as depicted on 3D TOF-MRA after the latency period.

Several studies have analyzed the ability of MR imaging and MRA to detect obliteration of the AVM nidus after radiosurgery (7, 8, 14–16, 21–24). Mukherji et al. (16) analyzed the sensitivity of 3D TOF-MRA to detect a small-volume AVM in 33 patients. These investigators reported a sensitivity of 27% and 50% for MIP and source images, respectively, for the detection of mean nidus diameters less than 1 cm. The low sensitivity may be due to low spatial resolution and weak flow signal obtained from a low field strength MRI system (1.0 T). Pollock et al. (22) analyzed the diagnostic accuracy of spin-echo MR imaging in comparison to conventional cerebral angiography to evaluate AVMs after radiosurgery in 164 patients. These investigators reported sensitivity of 80%, specificity of 100%, PPV of 100%, NPV of 84% and overall accuracy of 90% for the detection of a residual AVM. This difference of diagnostic performance between the use of contrast-enhanced 3D TOF-MRA and spin-echo MR imaging may be related to various factors such as the use of contrast media, spatial resolution of imaging techniques and the sizes of the residual AVMs.

Our study had several limitations. The study was not

designed to compare pre-contrast and post-contrast 3D TOF-MRA. A comparison between pre-contrast and post-contrast 3D TOF-MRA would allow easier differentiation of RIPE with abnormal vascular structures. Another limitation was the long follow-up interval between 3D TOF-MRA and X-ray angiography, up to six months.

In conclusion, contrast-enhanced 3D TOF-MRA at 3.0 T is highly sensitive but not highly specific for the detection of a small residual AVM after radiosurgery. Therefore, conventional X-ray angiography is still necessary to perform to confirm the status of an AVM after the latency period of radiosurgery.

References

1. Fleetwood IG, Steinberg GK. Arteriovenous malformations. *Lancet* 2002;359:863-873
2. Yamada S, Brauer FS, Colohan AR, Won DJ, Siddiqi J, Johnson WD, et al. Concept of arteriovenous malformation compartments and surgical management. *Neurol Res* 2004;26:288-300
3. Fournier D, TerBrugge KG, Willinsky R, Lasjaunias P, Montanera W. Endovascular treatment of intracerebral arteriovenous malformations: experience in 49 cases. *J Neurosurg* 1991;75:228-233
4. Lunsford LD, Kondziolka D, Flickinger JC, Bissonette DJ, Junqreis CA, Maitz AH, et al. Stereotactic radiosurgery for arteriovenous malformations of the brain. *J Neurosurg* 1991;75:512-524
5. Gobin YP, Laurent A, Merienne L, Schlienqer M, Aymard A, Houdart E, et al. Treatment of brain arteriovenous malformations by embolization and radiosurgery. *J Neurosurg* 1996;85:19-28
6. Schneider BF, Eberhard DA, Steiner LE. Histopathology of arteriovenous malformations after gamma knife radiosurgery. *J Neurosurg* 1997;87:352-357
7. Yamamoto M, Ide M, Jimbo M, Takakura K, Lindquist C, Steiner L. Neuroimaging studies of postobliteration nidus changes in cerebral arteriovenous malformations treated by gamma knife radiosurgery. *Surg Neurol* 1996;45:110-122
8. Yamamoto M, Jimbo M, Kobayashi M, Totoda C, Ide M, Tanaka N, et al. Long-term results of radiosurgery for arteriovenous malformation: neurodiagnostic imaging and histological studies of angiographically confirmed nidus obliteration. *Surg Neurol* 1992;37:219-230
9. Pollock BE, Lunsford LD, Kondziolka D, Maitz A, Flickinger JC. Patient outcomes after stereotactic radiosurgery for "operable" arteriovenous malformations. *Neurosurgery* 1994;35:1-7
10. Karlsson B, Lax I, Söderman M. Risk for hemorrhage during the 2-year latency period following gamma knife radiosurgery for arteriovenous malformations. *Int J Radiat Oncol Biol Phys* 2001;49:1045-1051
11. Maruyama K, Kawahara N, Shin M, Tago M, Kishimoto J, Kurita H, et al. The risk of hemorrhage after radiosurgery for cerebral arteriovenous malformations. *N Engl J Med* 2005;352:146-153
12. Kaufmann TJ, Huston J 3rd, Mandrekar JN, Schleck CD, Thielen KR, Kallmes DF. Complications of diagnostic cerebral angiography: evaluation of 19,826 consecutive patients. *Radiology* 2007;243:812-819
13. Heiserman JE, Dean BL, Hodak JA, Flom RA, Bird CR, Drayer BP, et al. Neurologic complications of cerebral angiography. *AJNR Am J Neuroradiol* 1994;15:1401-1407
14. Morikawa M, Numaguchi Y, Rigamonti D, Kuroiwa T, Rothman M, Zoarski G, et al. Radiosurgery for cerebral arteriovenous malformations: assessment of early phase magnetic resonance imaging and significance of gadolinium-DTPA enhancement. *Int J Radiat Oncol Biol Phys* 1996;34:663-675
15. Kauczor HU, Engenhart R, Layer G, Gamroth AH, Wowra B, Schad LR. 3D TOF MR angiography of cerebral arteriovenous malformations after radiosurgery. *J Comput Assist Tomogr* 1993;17:184-190
16. Mukherji SK, Quisling RG, Kubilis PS, Finn JP, Friedman WA. Intracranial arteriovenous malformations: quantitative analysis of magnitude contrast MR angiography versus gradient-echo MR imaging versus conventional angiography. *Radiology* 1995;196:187-193
17. Gauvrit JY, Oppenheim C, Nataf F, Naggara O, Trystram D, Munier T, et al. Three-dimensional dynamic magnetic resonance angiography for the evaluation of radiosurgically treated cerebral arteriovenous malformations. *Eur Radiol* 2006;16:583-591
18. Gaa J, Weidauer S, Requardt M, Kiefer B, Lanfermann H, Zanella FE. Comparison of intracranial 3D-TOF-MRA with and without parallel acquisition techniques at 1.5T and 3.0T: preliminary results. *Acta Radiol* 2004;45:327-332
19. Gibbs GF, Huston J 3rd, Bernstein MA, Riederer SJ, Brown RD Jr. Improved image quality of intracranial aneurysms: 3.0-T versus 1.5-T time-of-flight MR angiography. *AJNR Am J Neuroradiol* 2004;25:84-87
20. Hadizadeh DR, von Falkenhausen M, Gieseke J, Meyer B, Urbach H, Hoogeveen R, et al. Cerebral arteriovenous malformation: Spetzler-Martin classification at subsecond-temporal-resolution four-dimensional MR angiography compared with that at DSA. *Radiology* 2008;246:205-213
21. Nagaraja S, Lee KJ, Coley SC, Capener D, Walton L, Kemeny AA, et al. Stereotactic radiosurgery for brain arteriovenous malformations: quantitative MR assessment of nidal response at 1 year and angiographic factors predicting early obliteration. *Neuroradiology* 2006;48:821-829
22. Pollock BE, Kondziolka D, Flickinger JC, Patel AK, Bissonette DJ, Lunsford LD. Magnetic resonance imaging: an accurate method to evaluate arteriovenous malformations after stereotactic radiosurgery. *J Neurosurg* 1996;85:1044-1049
23. Kihlström L, Guo WY, Karlsson B, Lindquist C, Lindqvist M. Magnetic resonance imaging of obliterated arteriovenous malformations up to 23 years after radiosurgery. *J Neurosurg* 1997;86:589-593
24. Guo WY, Lindquist C, Karlsson B, Kihlstrom L, Steiner L. Gamma knife surgery of cerebral arteriovenous malformations: serial MR imaging studies after radiosurgery. *Int J Radiat Oncol Biol Phys* 1993;25:315-323